JOURNAL OF NANO- AND ELECTRONIC PHYSICS
Vol. 6 No 4, 04005(7pp) (2014)
ЖУРНАЛ НАНО- ТА ЕЛЕКТРОННОЇ ФІЗИКИ
Том 6 № 4, 04005(7cc) (2014)

Improvement of Front Side Contact by Light Induced Plating of c-Si Solar Cell

S. Maity[1,*], S. Dey[1], C.T. Bhunia[1], H. Saha[2]

[1] *Electronics and Communication Engineering, National Institute of Technology, 791112 Arunachal Pradesh, India*
[2] *Center of Excellence for Green Technology and Sensor Systems, IIEST, India -711103*

(Received 08 July 2014; revised manuscript received 27 November 2014; published online 29 November 2014)

Screen printing technique using silver paste is one of the established industrial processes for manufacturing solar cell. But due to some limitation of this process conductivity of contact decreases. Light Induced Plating (LIP) of c-Si solar cell is a critical process generally leading to decrease in series resistance of front side contact, increase in fill factor and efficiency associated with marginal reduction in short circuit current (*J*sc). In this paper experimental results showing the decrease in series resistance but increase in short circuit current (*J*sc) by using LIP process is reported. The LIP experiments are carried out using two different methods i.e. with and without bias. Even the unintentional deposition of silver nano particles on the front surface of the solar cell during LIP process is clearly shown.

Keywords: Solar cell, Silver nano particles, LIP, Air-voids, Plasmonic, Series resistance.

PACS number: 88.40.jp

1. INTRODUCTION

Firing step is playing an important role to achieve proper ohmic contacts in screen printing technique. Several factor arises during the screen printing technique, for example grid shading (~ 0.5 % loss), conductivity (~ 0.2 % loss), contact resistance (~ 0.2 % loss) etc which causes in reduction of solar cell efficiency [1]. Efficiency reduction is mainly due to inability to meet the requirement of narrower and thicker grid lines. During the annealing process conducting paste can be spread aside, thus its limits the aspect ratio at very low level [2]. The series resistance of Si solar cell varies because of gridline resistance, sheet resistance of the emitter and contact resistance between front emitter & electrode [6]. Sintering of Ag fingers produce a micro pores in plate, which reduces overall conductivity [5]. Till date many solutions have been reported in the literature to overcome the issues arising due to firing technique. Hilali and et al. have reported [7] that for better metal contact annealing has been done under forming gas atmosphere to enhance the fill-factor. Authors in [8] gave more as the need of oxygen for better adhesion of contact at the time of firing. The quality of the front side electrode for Si-solar cell is very important factor in regards to its performance. Photo lithographically designed front contact shows 0.5 % more efficient as compared to screen printing technology [9]. Because of its complexity and higher cost, this is not preferable for industry purpose. Therefore screen printing technique of silver paste emerges as the most cost effective and simple process for solar cell in large scale level. Some of the factors like grid shading, front surface recombination, density defect, etc cause poor conductivity leading to lower efficiency of solar cell [1]. Since the aspect ratio of screen printing silver reduces the efficiency by 0.5 %, therefore it needs to improve the aspect ratio of screen printed silver along with conductivity improvement for solar cell efficiency. Next generation screen printing applications rely on double printed contact lines (two layer metallization scheme) for achieving high aspect ratio and selective emitter technologies such as laser-doping [3]-[4],[10]-11] which reduce the electrical contact resistance. Electroless plating of Ni and Cu has also been successfully demonstrated in commercial production [12]. However, this technique involves high maintenance cost and times consuming process which limits its success [13-14]. Light induced plating (LIP) of silver has come out as an attractive method to improve the conductivity of the front side metallization [10-15]. The LIP technique was introduced in 1975 and it's quite different as it uses the solar cell ability to generate the photo current to drive the electrochemical deposition of the metal. After firing process, three current paths are formed between the bulk silver and the emitter [16]. Hence, the current movement is very high due to its lower resistance between them [17]. Fast plating rates, stability, lower cost and easy maintenance has made LIP simple and efficient. It is seen that LIP helps in improving the overall conductivity of the front side metallization not only by improving its thickness but also by filling up of voids in the screen printed silver. The voids are mainly formed when the organic solvent is removed during the drying process. More than a few works has been carried out by Lee et al. [18] and Bartesch et al. [13, 14] to estimate the efficiency gain by reducing optical shadowing losses.

In this paper, we mainly focused on the effect of LIP on the solar cell characteristics along with fill factor (FF) improvement and plasmonic effect related with LIP. In the proposed work, role of surface conditions and series resistance of front side contact after LIP has been examined. The unintentional deposition of silver nanoparticles on the surface of solar cell during LIP may lead to make changes in the Jsc of solar cell which could be caused by the plasma ionic effect [20].

2. EXPERIMENTAL

A suitable silver solution for proposed LIP experiment is preferred as this solution has cathode current

* santanumaity_4u@rediffmail.com

efficiency of 100 %. Three samples solution are taken by mixing different ratios of Potassium Argentum Cyanide (PAC) i.e. 5gm, 12.5 gm and 15 gm in 1000 ml de ionized (DI) water respectively. In light induced plating (LIP) experimental setup Silver (Ag) plate as anode and solar cell as cathode is chosen. In order to obtain the experimental result without bias p-side of solar cell is connected with anode (Ag-plate) and for bias setup (shown in fig. 1) an external supply that is constant current source of 5 mA is used respectively. Solar cell is placed horizontally at the bottom of the beaker and backside is protected by using poly tetrafluoro ethylene (PTFE) grid slab. The anode plate is placed around the solar cell in order to achieve maximum light intensity of 1000 W/m^2.

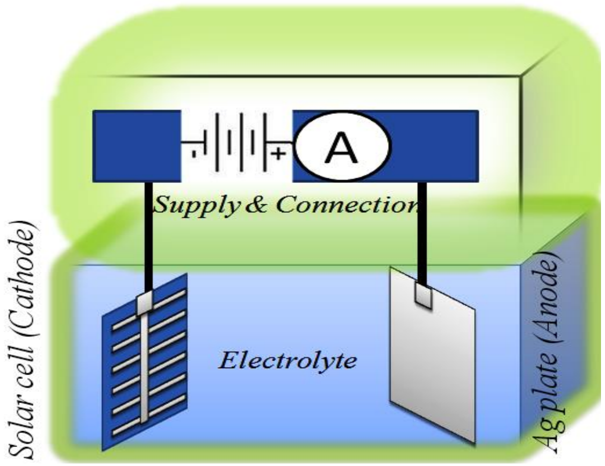

Fig. 1 – Simple representation of LIP at bias condition

The standard reaction in electrolyte state described bellow [4].

$$\mathrm{K}\left[\mathrm{Ag(CN)_2}\right] \rightarrow \mathrm{AgCN} + \mathrm{KCN}$$
$$\mathrm{AgCN} \rightarrow \mathrm{Ag^+} + \mathrm{CN^-}$$

Silver ion takes one electron from front printed contact and make Ag particle get deposited on front side contact. Also negative cyanide ion (CN-) moves to anode plate (silver plate) having positive silver ions (Ag$^+$) which reacts to give AgCN again The resulted AgCN reacts with KCN once again to yield PAC which maintaining the concentration of electrolyte solution constant.

$$\mathrm{Ag^+} + \mathrm{CN^-} \rightarrow \mathrm{AgCN}$$
$$\mathrm{AgCN} + \mathrm{KCN} \rightarrow \mathrm{K}\left[\mathrm{Ag(CN)_2}\right]$$

The I-V characteristic of the cell before and after LIP is measured using BENTHAM PVE300 Photovoltaic Device Characterisation System. From the I-V characteristics the solar cell parameters like current density (J_{sc}), open circuit voltage (V_{oc}), fill factor (FF), series resistance (R_s) and shunt resistance (R_{sh}) have been extracted using suitable software. The reflectance and External Quantum Efficiency (EQE) of each of the cells are also measured using BENTHAM PVE300 Photovoltaic Device Characterisation System. The possible deposition of silver nanoparticles on the surface of solar cell is investigated using Sigma series FESEM model from Zeiss. A new designed external bias set up of low cost circuital arrangement is shown in fig. 2. All the dotted line in fig. 2 shows the field line assumption inside the solution.

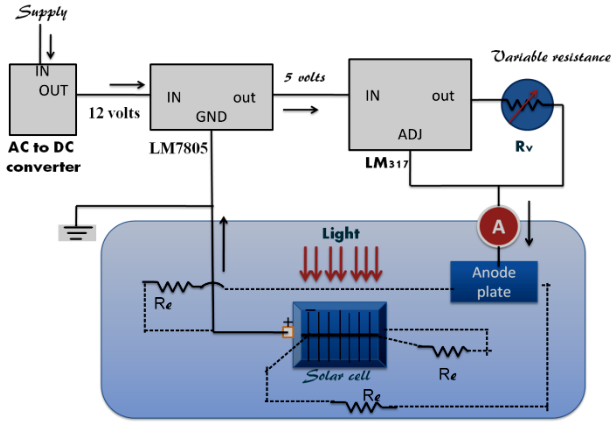

Fig. 2 – LIP circuit setup and inter electrolyte model

3. RESULT AND DISCUSSIONS

After hydrofluoric acid dipping it is seen that the fill factor (FF) increases gradually (shown in figure 3) where as the series resistance remains unchanged. But FF start decreasing if the solar cell is dipped HF solution for a time period 50 sec and more. This occurs due to lift off of the glass frit of front side contact. LIP experiment is carried out using different light intensities and different concentration of electrolyte solutions. Figure 4 and 5 shows that the series resistance of front side contact is decreasing with respect to time but it decreases rapidly for higher light intensity and higher concentration of solution within a limit otherwise optical shading occurs. During firing the solvent of silver paste used in screen printing process (SPP) evaporate making unwanted pores on the front side contacts which increases the series resistance therefore decreases the solar cell efficiency(as shown in fig. 6(a)). But after LIP process the pores get filled with silver particles as shown in fig. 6(b) reducing the series resistance and increasing the solar cell efficiency.

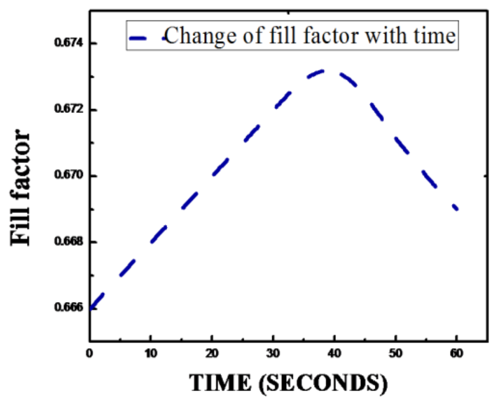

Fig. 3 – Change of fill factor depending on HF deeping

Considering l length finger lo is the void present in the finger (shown model 1). Now electric field $E = v / l$, here v is the applied potential and dv (where $-\mathrm{d}v = l\mathrm{d}R$) is potential drop at lo.

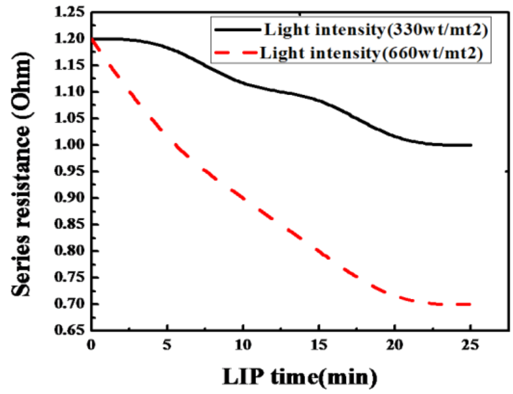

Fig. 4 – Series resistance change with light intensity

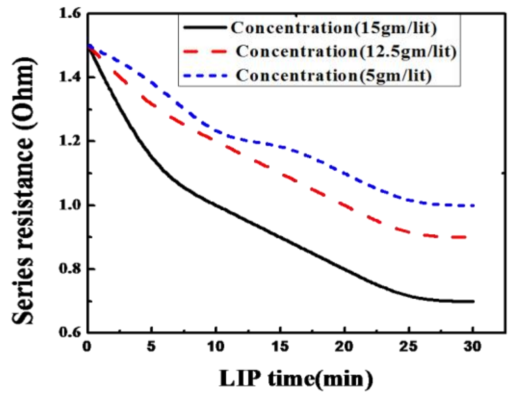

Fig. 5 – Series resistance change with concentration of solution

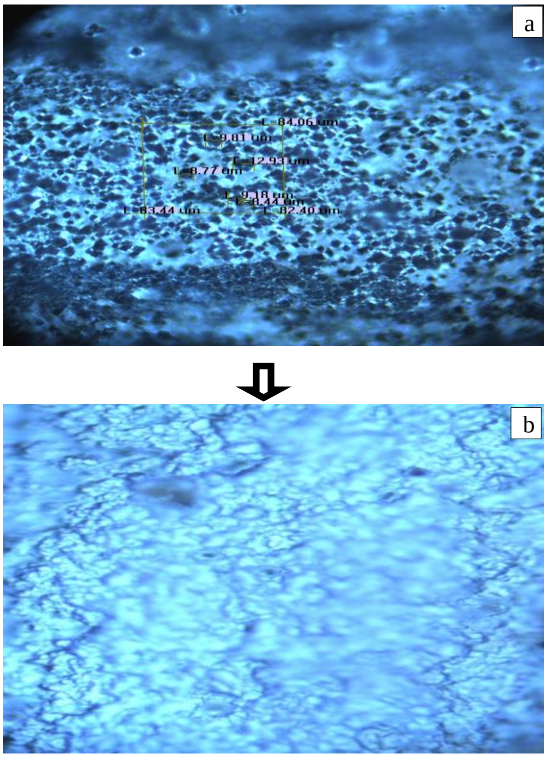

Fig. 6 – Microscopic view of solar cell contact (a) Microphot graph of finger before LIP (100X) (b) Microphotograph of finger after LIP (100X)

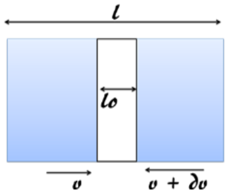

Model 1 – By taking single cut at contact

Now after taking l_0, electric field can written as $E = \upsilon_0 / l - l_0$. We know $J = \sigma E$ and $l = \sigma A$, $E = \sigma A \upsilon_0 / l - l_0$, from it is obtained $\upsilon_0 = I(l-l_0)/(A\sigma)$.

If the void portion is reduced to the second model then the generated resistance is written as

$$R = \rho\frac{l-l_0}{wt} + \rho\frac{l_0}{(w-b)t} =$$
$$= \frac{\rho}{t}\left(\frac{l-l_0}{w} + \frac{l_0}{w-b}\right)$$

Where ρ is the resistivity $d/2$ is the separation between the void bar and contact edge.

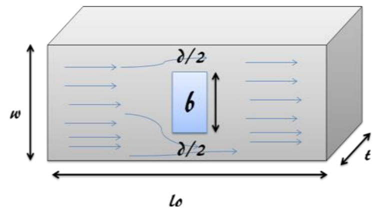

Model 2 – Reduced size of the cut

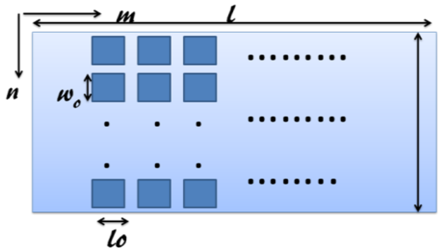

Model 3 – Distributed throughout the finger

Again n and m no of rows and columns are introduced to show the accurate result (shown model 3).

$$V_{grid} = \frac{(mn)(nw_0)t}{lwt} = (mn)\frac{l_0 w_0}{lw}$$
$$mn(l_0 w_0) = Vlw$$

$$R = \rho\frac{l-ml_0}{wt} + \rho\frac{ml_0}{(w-nw_0)t} =$$
$$= \frac{\rho}{t}\left[\frac{l-ml_0}{wt} + \frac{ml_0}{w-nw_0}\right] =$$
$$= \frac{\rho}{t}\frac{(l-ml_0)(w-nw_0)+ml_0 w}{w(w-nw_0)} =$$
$$= \frac{\rho}{w(w-nw_0)}\left(lw - ml_0 w - nlw_0 + nmw_0 l_0 + ml_0 w\right)$$

As $mnl_0w_0 = Vlw$

$$R = \frac{\rho}{wt(w - nw_0)}\left[l(w - nw_0) + Vlm\right] =$$

$$= \frac{\rho l}{wt(w - nw_0)}\left[(w - nw_0) + Vm\right] =$$

$$= \frac{\rho l}{wt}\left[1 + V\frac{w}{w - nw_0}\right] = R_0\left[1 - V\frac{w}{w - nw_0}\right]$$

Again by considering the voids are spherical and they are distributed haphazardly (shown model 4) on the contact then it can be modelled by GEMA approach

$$V_{air}\frac{\sigma_{air} - \sigma_e}{\sigma_{air} - \sigma_e} + (1 - V_{air})\frac{\sigma_{metal} - \sigma_e}{\sigma_{metal} - 2\sigma_e} = 0$$

If $V_{air} = 0$ then $\sigma_e = \sigma_{metal}$ and
$V_{air} = 1$ then $\sigma_e = \sigma_{air}$

If $\sigma_{air} \to 0$

$$-V_{air}\left(\frac{1}{2}\right) + (1 - V_{air})\frac{\sigma_{metal} - \sigma_e}{\sigma_{metal} - 2\sigma_e} = 0$$

$$\frac{\sigma_{metal} - \sigma_e}{\sigma_{metal} - 2\sigma_e} + \left(\frac{1}{2}\right) = V_{air}\left[\frac{\sigma_{metal} - \sigma_e}{\sigma_{metal} - 2\sigma_e} + \frac{1}{2}\right]$$

$$\sigma_{metal} - \sigma_e = V_{air}(3\sigma_{metal})$$

$$\sigma_e = \sigma_{metal}(1 - 3V_{air})$$

$$R = \rho\frac{1}{A} = \frac{1}{\sigma_{metal}(1 - 3V_{air})}\cdot\frac{1}{A}$$

$$\frac{1}{R} = \frac{\sigma_{metal}}{l}(1 - 3V_{air})A$$

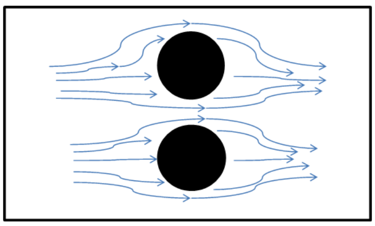

Model 4 – Spherical voids distribution

Again this model derived in different approach and analysis as bar of length L having some pores found during the time of firing is considered (as shown in figure 9). $W1$ and $W2$ is the width of the bar without considering the pore area. So, from the fig. 7, $W = W1 + W2 + \Delta L$ where ΔL is the diameter of the pore. Considering the pores distributed at X and Y axis randomly or for arbitrary distribution of pores a model equation can be derived as

$$R_{eff} = \frac{\rho L}{Wt}\left(1 + \frac{f_v}{1 - \Delta L/t}\right)$$

ρ = resistivity of bar; t = height of bar; f_v = void fraction.

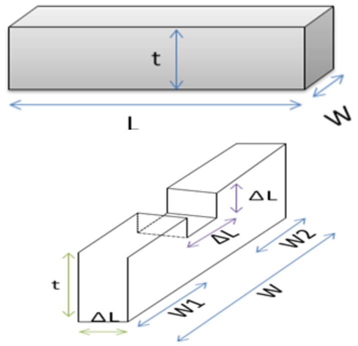

L – length of bar, W – with of the bar, t – thickness of the bar, ΔL – diameter of pore

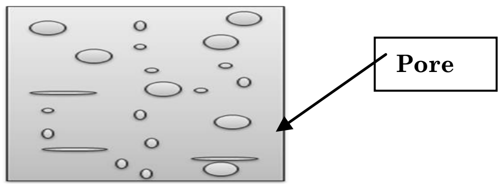

Fig. 7 – Model of finger with pore

Using the resultant model equation a MATLAB analysis is carried out by taking different values of pore diameter, void fraction, finger thickness and finger width. Finally on the basis of MATLAB analysis different graph are obtained between series resistance and different finger parameters as shown in fig. 8 to 11. From fig. 8 and 9 it can be seen that, the series resistance increases as the pore diameter and void fraction increases. As shown in fig. 10 and 11 due to increase finger thickness and width series resistance decreases.

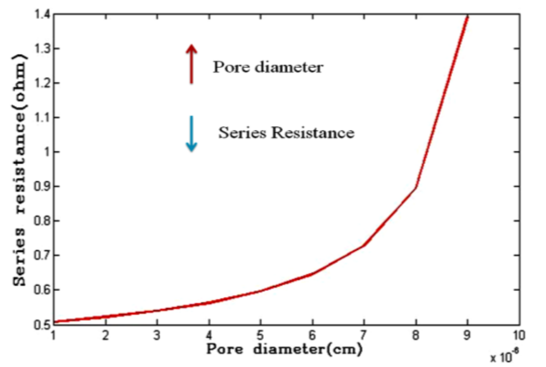

Fig. 8 – Series resistance changes with pore diameter

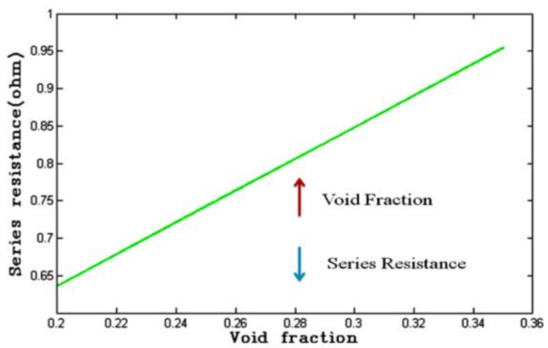

Fig. 9 – Series resistance vs void fraction

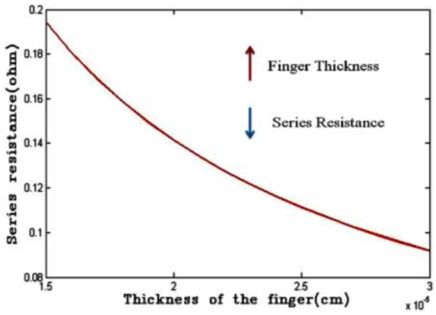

Fig. 10 – Series resistance changes with finger thickness

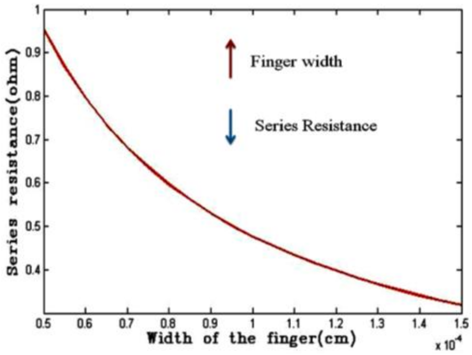

Fig. 11 – Series resistance vs finger width

3.1 LIP at with Bias Condition

From table 1 it can be seen that there is a significant increase of Jsc (21.3 mA/cm^2 to 26.06 mA/cm^2) while series resistance decreases (1.56 Ω to 1.47 Ω). However FF has decreased from 0.43 to 0.40 possibly due to reduction of Rsh from 26.7 Ω to 16.43 Ω. But from the spectral characteristic, it is noticed that there is a reasonable increases of EQE in the wavelength 500 nm to 900 nm. The behaviour of the spectral reflectance curves in figure 12 indicates that there may be a chance of unintentional deposition of different size nanoparticle all over the silicon solar cell surface which leads to plasmonic effect. This may be one of the possible reasons of increased Jsc and hence solar cell efficiency, although there is a small decrease of fill factor. On the other hand in the case of cell 2 J_{sc} has reduced significantly. The increase and decrease of Jsc can be

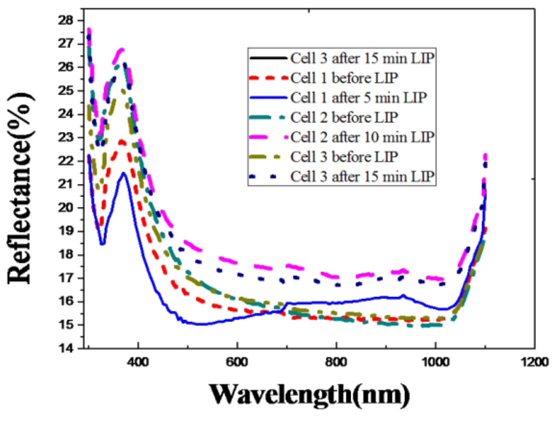

Fig. 12 – Reflectance of cells before and after LIP (with bias)

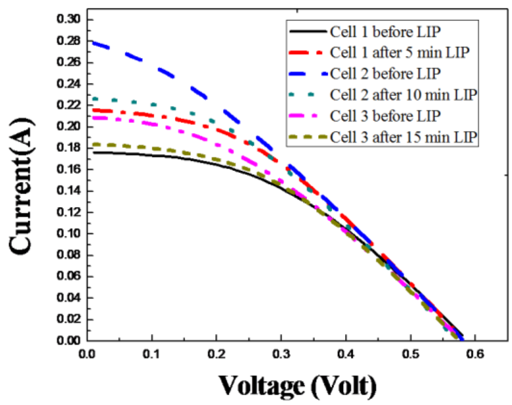

Fig. 13 – IV of cells before and after LIP (with bias)

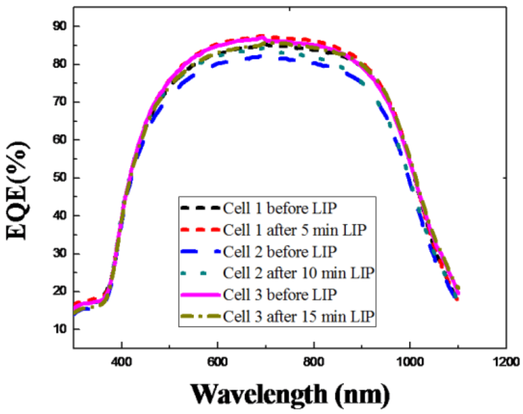

Fig. 14 – EQE of cells before and after LIP with bias

understood from External Quantum Efficiency characteristics of the cell as shown in the figure 13 and 14. This is may be due the increase of coverage of silver nano particle over the entire solar cell surface during LIP with a longer time 10 mins.

3.2 LIP at without Applied Bias Condition

In LIP without using external bias, a significant increase in J_{sc} (Figure 17) and reduction of reflectance (fig. 15)which may be one of the cause of efficiency improvement. Table 1 show that LIP without bias for 10 mins (Cell5) yield the best performance with respect to increase in Jsc and efficiency. From the spectral characteristic, it is noticed that there is a reasonable increase in EQE [Fig. 16] in entire region of light wave length from 300 nm to 1100 nm because of the increasing value of J_{sc} as shown in the illuminated IV characteristic curve (figure 17). So it can be concluded that if time of deposition is greater than 5 min and less than 15mins during LIP without bias is the optimized LIP parameters which got in experimental study.

FE-SEM image is taken using Sigma series of zesis, (shown in figure 19) showing the different size of silver nano particles deposited on bare surface of the solar cell. Solar cell without anti reflection coating is taken for LIP experimental study. As a result plasma ionic effect is introduced which improves the efficiency of solar cell by improving some parameters Jsc, EQE, IQE, and reflectance. But figure 18 shows nucleation of Ag particles due to longer time deposition which cause optical shading.

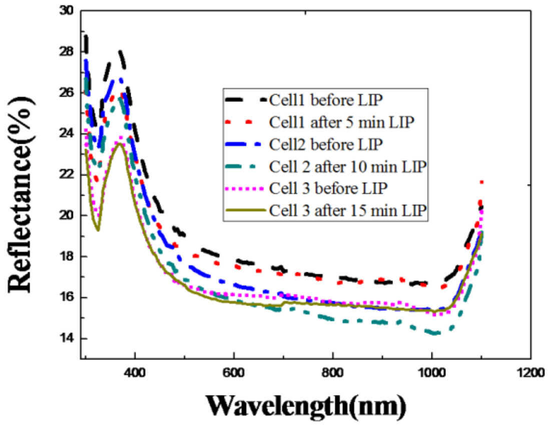

Fig. 15 – Reflectance of cells before and after LIP (without bias)

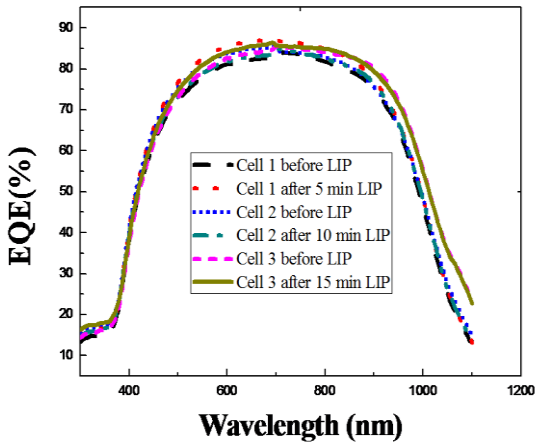

Fig. 16 – EQE of cells before and after LIP without bias

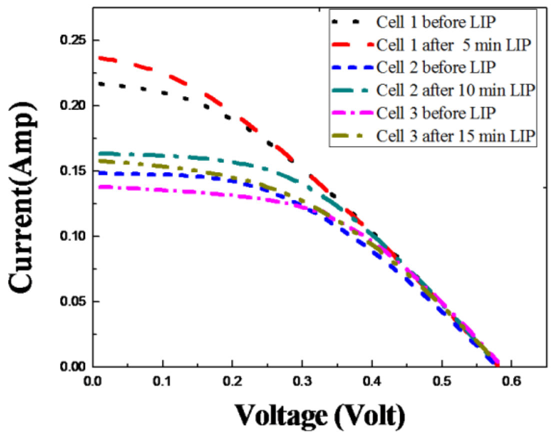

Fig. 17 – IV characteristics of cells before and after LIP without bias

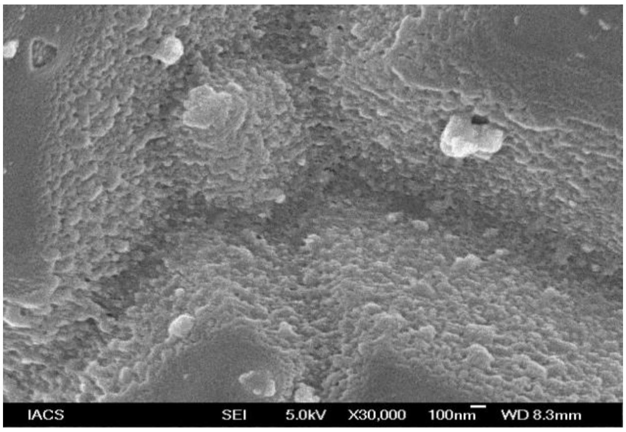

Fig. 18 – Nucleation due to over deposition

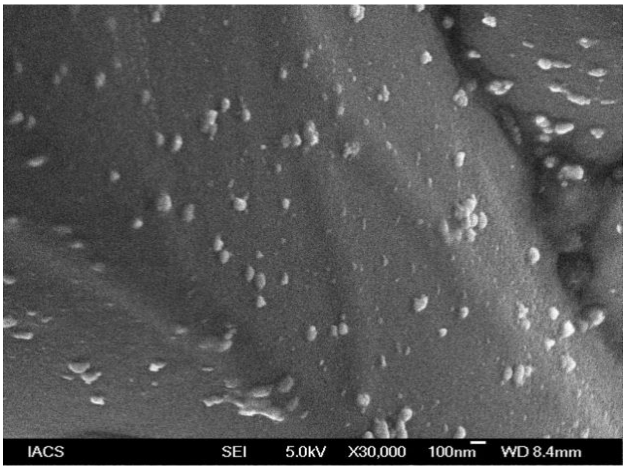

Fig. 19 – Deposited nanoparticles after LIP

4. CONCLUSION

For industrial application LIP is an established process for improving the *Rs* of the front contacts and reducing the shading loss in c-Si solar cell fabrication after screen printing technique. LIP is effective for unintentional improvement of contact resistance. In this paper experimental results are obtained by using two different chemical techniques concentrating not only on FF but also J_{sc}. Increase in J_{sc} and corresponding increase in efficiency without any significant change in FF is being reported. The unintentional deposition of silver nanoparticle on the surface of c-Si solar cell during LIP leads to a plasmonic effect which is an evidence showing reduction in the reflectance and increase of EQE of solar cell.

Table 1 – Different solar cell parameters at LIP with bias and without bias condition

567 wt/m²			WITH BIAS									
Sample no.	LIP time (Min)	Jsc (mA/cm²)	Area (cm²)	*V*oc (Volt)	*I*sc (mA)	*V*m (Volt)	*I*m (mA)	*P*m (mWatt)	*R*s (Ohm)	*R*sh (Ohm)	FF	η (%)
Cell 1B	5	5	8.25	0.58	176	0.340	129.20	43.92	1.56	26.70	0.43	9.38
Cell 1A				0.58	215	0.320	155.70	49.89	1.47	16.43	0.40	10.66
Cell 2B	10	5	9.9	0.58	278	0.310	165.50	51.29	1.54	4.58	0.32	9.19
Cell 2A				0.57	226	0.310	158.70	49.21	1.48	15.39	0.38	8.95
Cell 3B	15	5	8	0.57	208	0.320	140.60	44.98	1.58	14.76	0.37	9.67
Cell 3A				0.57	183	0.330	134.00	44.23	1.52	20.51	0.42	9.66
			WITH OUT BIAS									
Cell 4B	5	With-out bias	8.1	0.58	217	0.320	142.80	45.69	1.66	13.24	0.36	9.87
Cell 4A				0.58	237	0.310	147.17	45.62	1.72	8.62	0.33	9.88
Cell 5B	10	With-out bias	5.2	0.57	148	0.340	111.10	37.78	1.75	48.27	0.45	12.87
Cell 5A				0.58	164	0.340	126.90	43.16	1.59	38.28	0.45	14.52
Cell 6B	15	With-out bias	6	0.58	138	0.360	109.40	39.41	1.63	31.34	0.49	11.53
Cell 6A				0.56	158	0.350	112.40	39.34	1.71	20.48	0.43	11.6

ACKNOWLEDGEMENTS

We acknowledge two of our respected professors Dr. A.K. Barua and Dr. R. Bhattacharya for their constant support and encouragement. We extended our sincere gratitude to the Department of Science and Technology (DST), Government of India for their financial support in successes fully completing this work.

REFERENCES

1. Dr. Weiming Zhang, Vice President, *Technology*. *Heraeus Materials Technology LLC "How Silver Paste Improve Silicon Solar Cell Performance/Cost Ratio*. http://heraeus-pvsilverpaste.com.
2. Xing Zhao, et al., *J. Semiconductors* **33** No 9, 094008 (2012).
3. L. Mai, et al., *34th IEEE Photovoltaic Specialists Conference, 1811* (7-12 June: Philadelphia, PA: 2009).
4. A. Sugianto, et al., *35th IEEE Photovoltaic Specialists Conference, 689* (20-25 June: Honolulu, HI: 2010).
5. Mattmoynihan, *An over view of wet chemistry processing for the manufacture of silicon solar cell,* Article 42515335, **22** No 7, 16, (2009).
6. J.H. Lee, Y.H. Lee, J.Y. Ahn, et al., *Sol. Energ. Mat. Sol. C.* **95**, 22 (2011).
7. M. Hilali, *Understanding and development of manufacturable screen-printed contacts on high sheet resistance emitters for low cost silicon solar cells*. Ph.D thesis, Georgia Tech (2005).
8. G. Cheek, R. Mertens, R. Van Overstraeten, L. Frisson, *IEEE T. Electron. Dev.* **ED-31** No 5, 602 (1984).
9. Ansgar Mette, *New concepts for front side metallization of industrial silicon solar cells*. PhD thesis, Fraunhofer-ISE.
10. B.S. Tjahjono, et al., *Proc. 22nd European Photovoltaic Solar Energy Conference, 966* (Milan: Italy: 2007).
11. D. Kray, et al., *Proc. 35th IEEE Photovoltaic Specialists Conference, 667* (Honolulu, HI: 2010).
12. N.B. Mason, et al., *Proc. 17th European Photovoltaic Solar Energy Conference, 227* (Rome, Italy: 2002).
13. J. Bartsch, et al., *J. Appl. Electrochem*. **40**, 757 (2010).
14. J. Bartsch, et al., *Proc. 24th European Photovoltaic Solar Energy Conference, 1469* (Hamburg, Germany: 2009).
15. L.F. Durkee, *Method of plating by means of light*, 4144139, United States (1979).
16. D. Pysch, A. Mette, A. Filipovic, et al. *Prog. Photovoltaic.: Res. Appl.* **17** No 2, 101 (2009).
17. Xing Zhao, Jia Rui, Ding Wuchang, Meng Yanlong, Jin Zhi, Liu Xinyu, *J. Semiconductors* **33** No 9, 094008 (2012).
18. Jin Hyung Lee, Young Hyung Lee,Jun Yong Ahn, Ji-Weon Jeong, *Sol. Energ. Mater. Sol. C.* **95**, 22 (2011).
19. Y. Yaon, A. Sugianto, A.J. Lennon, B.S. Tjahjono, S.R. Wenham, *Sol. Energ. Mater. Sol. C.* **96**, 257 (2012).
20. Santanu Maity, Sonali Das, Swapan Datta, Hiranmay Saha, Soma Ray, Utpal Gangopadhyay, *Plasmonic effect in Light-Induced Plating of c-Si solar cell* ICEE (2012).